



HAL
open science

Comparative comminution efficiencies of rotary, stirred and vibrating ball-mills for the production of ultrafine biomass powders

Karine Rova Rajaonarivony, Claire Mayer-Laigle, Bruno Piriou, Xavier Rouau

► To cite this version:

Karine Rova Rajaonarivony, Claire Mayer-Laigle, Bruno Piriou, Xavier Rouau. Comparative comminution efficiencies of rotary, stirred and vibrating ball-mills for the production of ultrafine biomass powders. *Energy*, 2021, 227, pp.120508. 10.1016/j.energy.2021.120508 . hal-03259300

HAL Id: hal-03259300

<https://hal.inrae.fr/hal-03259300>

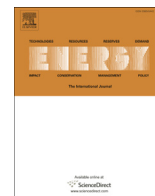
Submitted on 14 Jun 2021

HAL is a multi-disciplinary open access archive for the deposit and dissemination of scientific research documents, whether they are published or not. The documents may come from teaching and research institutions in France or abroad, or from public or private research centers.

L'archive ouverte pluridisciplinaire **HAL**, est destinée au dépôt et à la diffusion de documents scientifiques de niveau recherche, publiés ou non, émanant des établissements d'enseignement et de recherche français ou étrangers, des laboratoires publics ou privés.



Distributed under a Creative Commons Attribution - NonCommercial - NoDerivatives 4.0 International License



Comparative comminution efficiencies of rotary, stirred and vibrating ball-mills for the production of ultrafine biomass powders



Karine Rova Rajaonarivony^a, Claire Mayer-Laigle^{a,*}, Bruno Piriou^b, Xavier Rouau^a

^a IATE, Université de Montpellier, CIRAD, INRAE, Montpellier SupAgro, 34060, Montpellier, France

^b BioWooEB, Université de Montpellier, CIRAD, TA B-114/16, 73 Rue Jean-François Breton, 34398, Montpellier, France

ARTICLE INFO

Article history:

Received 9 December 2020

Received in revised form

25 March 2021

Accepted 27 March 2021

Available online 1 April 2021

Keywords:

Mechanical stress

Fine comminution

Ball mill

Energy

Lignocellulosic biomass

Powder

ABSTRACT

Plant biomass as a substitute for fossil oil is one of the most promising pathways to reducing the environmental impact of human activities. Ultrafine comminution of plant materials can produce ultrafine powders suitable for direct use in advanced-technology applications as an engine, becoming a sustainable powdered biofuel. However, comminution is an extremely energy-intensive process, making it vital for industry to select the most efficient milling device for the biomass. Here, we comprehensively compared the efficiencies of three batch ball mills employable for ultra-fine comminution of plant materials. First, we led a ball motion study to estimate the predominant mechanical stresses generated by each device. Two biomasses with contrasted physical properties were milled using three devices to achieve a target particle size of 20 μm . Milling times and process energy consumption were recorded, and the particle size distributions and specific surface areas of the ground powders were measured. The balls mills were then compared based on several indicators of energy efficiency, productivity and processing speed. The results show that the energy input is better utilized in mills that work by attrition or by combined impact and attrition.

© 2021 The Authors. Published by Elsevier Ltd. This is an open access article under the CC BY-NC-ND license (<http://creativecommons.org/licenses/by-nc-nd/4.0/>).

1. Introduction

Efficient use of natural renewable resources for clean and affordable energy is one of the United Nations Sustainable Development Goals (SDGs) on the 2030 Agenda [1]. It is also part of core International Energy Agency policy to increase the share of biomass energy from 10% to 30% by 2050 [2]. A key to achieving these targets would be to increase the proportion of biofuels used in transportation and in stationary engines for electricity generation. However, second-generation liquid and gas biofuels struggle to deliver profitable margins, chiefly due to limitations on upstream logistics concerning centralized sourcing and processing, and transport for distribution [3,4].

Another alternative and technically straightforward approach is to directly use of lignocellulosic biomass in the form of finely-pulverized dry powders, for example as a substrate for high-performance gasification and advanced liquefaction technologies [5], or even to as a micronized dry biomass fuel to directly power internal combustion engines [6–9]. This potentially valuable

concept relies on the fact that when used in suitable quantity and concentration in a confined environment, finely-milled biomass undergoes rapid combustion in the form of a deflagration [10]. The violence and speed of the explosion are linked to size and composition of the particles. The energy released by the explosion depends on degree of confinement and heat losses [11], and it can be recovered as mechanical force if the explosion is controlled and takes place in a combustion engine. Engines of different power levels are in widespread use for a huge number of mobile and stationary applications in areas that are potentially rich in under-utilized biomass feedstocks. This kind of a technology would enable small-scale on-site energy generation with minimal processing complexity.

Lignocellulosic biomass consists of various plant portions of different origins and compositions but that sharing an elastoplastic mechanical behaviour that makes it hard and energy-intensive to finely mill. Firm process control of the milling step is therefore a pivotal challenge for the development of ultrafine biomass technologies, for two main reasons. First, fine milling has to be optimized to keep solid fuel production and utilization energetically profitable [12]. The optimization needs to be done in conjunction with the target biomass, as its energy content and milling energy

* Corresponding author.

E-mail address: claire.mayer@inrae.fr (C. Mayer-Laigle).

Symbols and abbreviations

Es	Specific energy consumption
Ec	Maximum kinetic Energy of moving bodies in the ball mills
IM	Impact mill
Pm	Mass productivity
RBM	Rotary ball mill
Rs	Surface creation rate
S _{ball}	Geometric Surface of milling bodies
SSA _i , SSA _t , SSA _f , SSA _{granulo} , SSA _{BET}	Specific surface area –initial, total, final, measured by granulometry, measured by BET method
SBM	Stirred ball mill
ts	Specific milling time
Ue	Energy utilization
VBM	Vibratory ball mill

demand are directly connected to its chemical and physical properties. Second, the interactions between milling parameters and type of biomass feedstock also determine the end-use quality of solid fuel powder, as the particle size reduction improves its reactivity and influences its handling properties.

Biomass can be either dry-milled or wet-milled, but dry milling precludes the need for a final drying step, does not produce effluents, and has no solubilization-related losses, making it a preferable option, especially for energy-process applications. In addition, the devices employed for dry milling are relatively basic, the feedstock being milled only by the mechanical energy brought by a milling tool or by the motion of milling media. However, regardless of the configuration and geometry employed, there is still no mill solution that can convert directly most of current lignocellulosic material feedstocks into very fine powders. The process of particle size reduction has to be progressive and will generally entail several milling steps using different grinding principles: cutting mills for initial coarse size reduction (from cm to mm range), impact mills for intermediate grinding (from mm to 100 μm range), and ball or jet mills for fine and ultrafine milling (50–10 μm range). Here we will not discuss the sophisticated and energy-intensive air-jet milling process, which in practice is limited to high-added-value products, but rather the different ball-milling configurations that are better adapted to real-world biomass process routes. Milling energy consumption is directly related to the extent of particle size reduction, with the final pulverization step being the most energy intensive [13]. However, energy consumption depends on both the material to grind [14–16] (related to its initial size, water content, intrinsic mechanical properties linked to its composition, its structure and any pre-treatments) and the efficiency of the milling machine [14,17–21] (related to its working principle, mechanical stress, and process scalability).

Fragmentation of the material matrix is effectuated by the mechanical stresses applied inside the mills. Four main mechanical stresses are generally identified: compression, shear, impact, and attrition [17]. These different mechanisms all co-exist in most the milling machines, but mill geometries and processing parameters will mean that one mechanism generally dominates the others. To reach the fine and ultrafine domains of particle sizes (median particle size <50 μm), Rajaonarivony et al. [3] showed in a model study using a small-scale ball mill on pine bark that impact is more energy-efficient mechanical stress during the first stage of the

fragmentation process whereas attrition becomes more efficient when the average particle population reaches the ultrafine domain. They concluded that a unit operation combining first impact then attrition was the most effective mechanical stress sequence for the ultrafine comminution of this biomass. On a larger scale, industrial drum-type ball-mills tend to rely on impact as the dominant comminution stress. However, an increasing contribution of attrition should be sought as particle get smaller. This can be achieved, for example, in stirred bead mills [22] or vibratory finishing mills [5]. Thus, identifying the most energy-efficient mill geometry and operating parameters to reach targeted powder specifications is a key part of the challenge to optimize lignocellulosic biomass utilization.

Here we explore the energy performances of ball mills for extensive particle size reduction on two lignocellulosic biomasses of contrasting types (pine bark, which is a fragile layered material, and wheat straw, which is a tenacious fibrous material). Target particle size was set at 20 μm , to allow direct use of the feedstock for energy in high power applications. The experimental setup was designed to account for the specificity of elastoplastic materials like lignocellulosic biomasses [23] and to highlight the energy consumption difference that may arise from wide range of plant material types. We compared three different ball-mill setups (rotary-drum mill, RBM; stirring-rotor mill, SBM; vibratory ball mill, VBM) that can be used for fine comminution of lignocellulosic materials [5,23–25] in an attempt to correlate the mechanical stresses generated with comminution processing efficiency. The original contribution of this work is that for the first time, we directly compare three milling technologies used for dry processing of lignocellulosic biomass to attain very fine particle sizes. We anticipate this analysis of mill function, milling energy and processing speed as valuable input to help industry select and scale more efficient equipment for the fine comminution of various biomasses.

2. Materials & methods

2.1. Materials: presentation of the two biomasses

The lignocellulosic biomasses used in this study are maritime pine bark (*Pinus pinaster*) and wheat straw (*Triticum aestivum*). The maritime pine bark was purchased from a local store (Botanic, Montpellier, France) in 35-kg bags, and was size-calibrated to 10–25 mm-length pieces. Moisture content of the bark, which depends on storage conditions, was 35–40%. To reduce its water content below 15% before milling, the bark was dried outdoors for 48h. The wheat straw was harvested in 2015 at Saint-Gilles (Gard, France) and delivered as 25-kg bales. Initial moisture content of the wheat straw was 11%.

Moisture content was measured by weight loss after oven-drying for 2 h at 135 °C according to standard protocol for cereal flours and lignocellulosic products [26].

2.2. Preparation of the plant material

Prior to the fine milling unit operation which is the focus of this study, both plant materials were pre-milled in two steps. First, a Retsch SM 300 knife mill with a 2 mm-aperture sieving grid was used to grind the samples, which were then dried in an oven at 60 °C to reach 3% moisture content. Second, the samples were run through an impact mill (IM) (UPZ 100 Hosakawa-Alpine, Germany) equipped with a 0.3-mm sieving grid at a feed rate of 1.5 $\text{kg}\cdot\text{h}^{-1}$ (Fig. 1). The resulting powders, named IM_bark and IM_straw, had a median particle size measured by laser diffraction (see section 2.4 for particle size analysis) of 63 μm and 286 μm , respectively. Apparent density of each powder was determined by simply



Fig. 1. Milling devices used: (a) knife mill, (b) impact mill (IM), (c) rotary ball mill (RBM), (d) stirred ball mill (SBM), and (e) vibratory ball mill (VBM).

weighing a known volume of powder slightly packed after tapping 5 times to homogenize the powder bed. The apparent density values obtained were $381 \text{ kg}\cdot\text{m}^{-3}$ for IM_bark and $191 \text{ kg}\cdot\text{m}^{-3}$ for IM_straw.

Before final comminution in the different ball mills, all samples were re-dried to a moisture content of about 3%, as measured by weight loss after oven-drying for 2 h at $135 \text{ }^{\circ}\text{C}$.

2.3. Fine comminution with the different ball mills

The three types of ball mill (RBM, SBM, VBM) were employed for the fine comminution of bark and straw to obtain powders with a median particle size of $20 \mu\text{m}$ (Fig. 1). The samples were directly mixed with the balls inside the milling chambers of each mill. All mills used in this work are batch mills. At the end of milling, the ground powders were separated from the milling media by dry sifting. The different milling devices employed here do not work at exactly the same scale and are not based on the same principles, and so volume of the milling chambers, weight of the milling media, and weight and volume of the biomass may differ between mills. The milling parameters for each device are described below and in Table 1. They were defined according to suppliers' specifications and from extensive preliminary works on biomass milling, as described in a data paper [25].

The *rotary ball mill* (RBM, Faure, France) consists of a ball-filled drum fixed on two rollers that impart a rotational movement to the drum. The milling media are steel balls of three diameters (25, 20 and 15 mm) combined in a 1:1:1 ratio by mass. The milling media fill one third of the total volume of the drum. Rotary speed was set to 60 rpm in order to induce a cataracting regime for the balls [17,27]. The *vibratory ball mill* (VBM, Sweco, Belgium) consists of a 36 L-capacity grinding chamber made of an abrasion-resistant elastomer, put in vibrating motion by high-tensile steel springs [28]. Vibratory frequency of the vessel was set to 25 Hz, as per the manufacturer's recommendations. Amplitude of the vibrations is a function of the whole charge of the chamber and the stiffness of the springs. The milling media employed is a blend of 25 kg of ceramic cylpebs (cylindrical bodies of 12-mm length and 12-mm diameter) and 25 kg of ceramic beads (12-mm diameter). In charge, the amplitude of vessel displacement was 2.5 mm (optical measurement). The *stirred ball mill* (SBM) is a custom-made prototype (IATE, INRAE, France) that consists of a 2 L-capacity grinding chamber in which a rotor operating at 330 rpm drives the milling media (5.7 kg of 6-mm-diameter steel beads) mixed with the powder to grind. All operating process parameters are summarized in Table 1. For this work, we elected to operate the different milling devices using the same mass but not the same volume. As the energy content of biomass is proportional to its mass, its volume evolves during the

Table 1
Process parameters used in the three ball mills for fine comminution of bark and straw.

	RBM	VBM	SBM
Speed/Frequency	60 rpm	25 Hz	330 rpm
Ball dimensions (mm)	Ø 25 - 20 -15 mm	beads: Ø 12 mm cylpebs: Ø 12 mm and length 12 mm	Ø 6 mm
Volume of the vessel (L)	2	36	3
Diameter of the vessel (cm)	17.5	N/A	16
Mass of samples (kg)	0.2	1.0	0.325
Mass of milling balls (kg)	3	50	5.7
	Biomass volume fill rate (%)		
Bark	26	7	29
Straw	53	15	58
	Total (biomass + milling media) volume fill rate (%)		
Bark	46	42	49
Straw	73	52	83

milling process as particle size decreases, which means that in practice, it is easier to manage the mass than the volume, especially when the process is fed with several feedstock sources. As there is a two-fold difference between the apparent densities of two raw powders (IM_bark and IM_straw), the biomass fill rate and total volume fill rate differ significantly between the two biomasses.

Milling experiments in the three milling devices were conducted in duplicate. A first set of experiments was conducted with sampling at regular intervals throughout milling to determine the milling time necessary to reach the target particle size of 20 µm for each biomass in each milling device. Then, a second set of milling experiments was conducted using the milling times thus determined, and the final particle size was measured. Finally, we calculated the coefficients of variation between the $SSA_{granulo}$ of the two experiments to evaluate the reproducibility of this milling step.

The output data from the different milling experiments were milling time, energy consumption of the devices, the particle size distribution and specific surface area of the ground powders, which was determined from particle size distribution and BET-method measurements. The different methods employed are described below.

2.4. Particle size analysis

Particle size distribution (PSD) was measured in dry way with a Mastersizer 2000 laser diffraction granulometer (Malvern, UK) equipped with a Sirocco 200 feed hopper [29]. The amplitude of the feeder vibration was set to 50% of the maximal value, and air pressure was set to 3 bars. In this configuration, the mass of the analyzed samples was around 2 g. All measurements were carried out in duplicate and averaged. Results were expressed in volume, based on the assumption of sphere-shaped particles. The 10th (d10), 50th (median particle size: d50) and 90th (d90) percentiles and the specific surface area (denoted $SSA_{granulo}$) were extracted from the particle size distributions.

2.5. Specific surface area measurement with the BET method

This method is based on the principle of measuring gas sorption onto the surface of the particles. Here, the measurements were performed using nitrogen. First, 1.5–2 g samples of raw powders (IM_bark and IM_straw) and 1–1.5 g samples of finely milled powders were degassed for 48 h at 50 °C using a Vacprep 061 degasser (Micrometrics, USA) to remove moisture and other adsorbed molecules. Samples were then analyzed using an ASAP 2460 Analyzer (Micrometrics, USA). Sorption isotherms were recorded with 12 relative pressures p/p^0 varying between 0.05 and 0.35. Specific surface area was determined using the BET method applied on the linear part of the Rouquerol plot [30]. All BET

measurements were carried out in duplicate. The resulting data were written as SSA_{BET} .

2.6. Energy

2.6.1. Maximum kinetic energy of the moving bodies

Here, we propose a methodology to highlight the predominant mechanical stresses based on the maximum kinetic energy of the moving bodies. The calculation includes several approximations and is not intended to give exact values of the energy delivered to the powder by mill, but rather to give orders of magnitude that can serve to cross-compare the milling devices. The maximum kinetic energy that one moving body can reach (E_c) was estimated from its mass (m) and maximum velocity (v) during a collision (eq. (1)). The maximum total kinetic energy (E_{ct}) was obtained by multiplying the maximum velocity of one moving body (v) by the total mass of the moving bodies (m_t).

$$E_c = \frac{1}{2}mv^2 \text{ and } E_{ct} = \frac{1}{2}m_tv^2 \quad \text{Eq.1}$$

In the RBM, maximum velocity (v) was calculated from the velocity that a moving body can reach when free-falling across the diameter (d) of the drum (eq. (2)), with g as gravitational acceleration. In this case, m is the mass of a 25-mm-diameter ball.

$$v_{RBM} = \sqrt{2gd} \quad \text{Eq.2}$$

In the VBM, maximum velocity was estimated from the amplitude of displacement of one moving body and vibrational frequency (f) (eq. (3)), and m is equal to the mass of one moving body.

$$v_{VBM} = af \quad \text{Eq.3}$$

In the SBM, maximum velocity was assimilated to maximum peripheral rotor speed (eq. (4)), and m is equal to the mass of one moving body (6-mm-diameter steel ball).

$$v_{SBM} = \omega \frac{D}{2} \quad \text{Eq.4}$$

where ω is rotor velocity and D is rotor diameter.

Note that in practice, maximum velocity and maximum kinetic energy can never be reached in any of the ball mills devices. The aim of these calculations is simply to determine the total energy limit of the milling bodies for each mill.

2.6.2. Milling energy consumption

For all experiments, the power of the milling devices was measured using a PX 120 wattmeter (METRIX, France) connected to WattCom (USA) data acquisition software, and the mean power

over the total duration of the experiments was calculated. Milling energy consumption was determined by multiplying mean power by total milling time, and then used to compute various energy-use indicators:

2.6.2.1. - Specific energy consumption. Specific energy consumption (E_s) (eq. (5)) was calculated with equation (5), where P is power of the milling device (in watts), m_{sample} is processed mass (in tons), and t is grinding time (in seconds):

$$E_s = \frac{P t}{m_{\text{sample}}} \quad \text{Eq.5}$$

2.6.2.2. - Specific milling time. Specific milling time is the time needed to produce 1 kg of lignocellulosic biomass powder with $d_{50} = 20 \mu\text{m}$. Specific milling time is obtained by dividing actual milling time by the mass processed (m_{sample}):

$$t_s = \frac{t}{m_{\text{sample}}} \quad \text{Eq.6}$$

where t is the actual milling time needed to mill the actual processed mass of sample (m_{sample}).

2.6.2.3. - Energy utilization. Energy utilization (U_e) (eq. (7)) is the ratio of specific surface created to specific energy consumption (E_s). It expresses the specific milling work of the comminution process [24]:

$$U_e = \frac{SSA_f - SSA_i}{E_s} \quad \text{Eq.7}$$

where SSA_i and SSA_f are initial and final specific surface area, respectively (*i.e.* before and after milling). U_e values were determined from both SSA_{granulo} and SSA_{BET} .

2.6.2.4. - Mass productivity. Mass productivity (P_m) is defined here as the mass of powder with a median particle size (d_{50}) of $20 \mu\text{m}$ produced by the milling device with an energy input of 1 kWh. It is calculated using the equation (8):

$$P_m = \frac{m_{\text{sample}}}{E_s} \quad \text{Eq. 8}$$

2.6.2.5. - Surface creation rate. Surface creation rate (R_s) (eq. (9)) is defined here as the increase in SSA_{BET} generated by 1 h of milling, which corresponds to the speed of surface creation:

$$R_s = \frac{SSA_f - SSA_i}{E_s} \quad \text{Eq. 9}$$

2.6.2.6. - Lower heating value of the biomass samples. The lower heating values of bark and straw were measured in a bomb calorimeter as protocolled in standard XP CENT/TS 14918 [31].

3. Results

The scientific literature has given many definitions of milling efficiency according to purpose of the study and application targeted [32]. Here we explored several of these definitions from different viewpoints. In a first approach, the performance of the

three milling devices was evaluated on the basis of two parameters: (i) specific milling time, which is the time required to produce 1 kg of fine lignocellulosic biomass powder, and (ii) specific energy consumption, defined as the amount of energy needed to mill 1 ton of biomass to the targeted particle size of $20 \mu\text{m}$. These two indicators have the advantage of directly addressing the practical industrial issues of time and energy consumption required to obtain a powder meeting the required specifications. Then, in effort to gain a more in-depth analysis taking into account the difference between particle in-feed sizes and to overcome the dependency on capacity differentials between the ball-mill devices, we introduced a further indicator of grindability based on the Rittinger model. Finally, the metric of energy utilization introduced by Mucci & R acz (2017) [24] was calculated from specific surface area based on either laser diffraction or BET-method measurements to capture the influence of the fine particles on agglomeration and the efficiency of the comminution process. All the data are discussed in relation to the dominant mechanical stress in each device, as presented below.

3.1. Dominant mechanical stresses in the three ball-milling devices

Table 2 summarizes the maximum energies that the ball media were able to deliver (as the sum of the individual energy limit of the milling bodies in each ball mill calculated from their weight and their theoretical maximum velocity in a standalone frictionless setting) and the surface ratio between the milling bodies and the biomass samples, in an attempt to determine the main mechanical stresses applied by the three ball-mill types.

The total surface of the milling bodies was calculated from their size and shape, and total surface of the biomass samples was obtained by integrating the particle size distribution curve measured by laser granulometry. The maximum kinetic energies of the milling media were calculated for each milling device.

Note that the RBM delivered by far the highest energy of a single ball, due to the higher mass of the balls used (steel balls with 25/20/15-mm diameters) and a significant free-falling distance. The VBM imparted very little energy *via* each ceramic ball or clypebs due to the very short length of amplitude (2.5 mm). The SBM delivered an intermediate amount of energy through each relatively small (6-mm-diameter) steel ball, due to the high speed conferred by the driving rotor. However, when considering the total amount of milling bodies, *i.e.* the maximum total kinetic energy delivered by each mill, SBM emerged as 3-times more energy-intensive than RBM and 170-times more energy-intensive than VBM.

Another parameter to account for when comparing the mechanical stresses in the different mills is the ratio of milling body surfaces to biomass surfaces, which describes the potential number of contacts between milling bodies and the material to mill. This surface ratio is directly related to biomass volume fill rate and is different between bark and straw due to their differences in feed-particle sizes and apparent densities ($381 \text{ m}^3.\text{kg}^{-1}$ for bark vs. $191 \text{ m}^3.\text{kg}^{-1}$ for straw). Straw feed particles are larger than bark feed particles, and at equal the bark and straw masses, straw feed sample volume is twice as big as bark feed sample volume. Therefore, straw induces a higher ball-to-biomass surface ratio due to a lower proportion of lignocellulosic matter. Among the three mills, RBM delivered the fewest milling body-to-milled matter contacts whereas VBM delivered the most contacts, with SBM again intermediate between RBM and VBM although closer to VBM.

Finally, we calculated the ratio of total kinetic energy to surface available per kg of sample material in order to factor in the different amounts of treated matter in each batch. The aim here was to compare the different mills on a comparable basis. The RBM was

Table 2
Kinetic energy of the ball media and ball-to-biomass matter surface contact points in the three ball mills, used to determine their major mechanical stresses.

	RBM		SBM		VBM	
	Bark	Straw	Bark	Straw	Bark	Straw
Maximum kinetic energy delivered by one milling body (kWh. 10 ⁻⁸)	1500		96		0.33	
Maximum kinetic energy delivered by the whole milling media (kWh .10 ⁵)	182		627		3.7	
Ball-to-matter surface ratio $S_{ball}/S_{sample} \cdot 10^{-3}$	2	10	8	30	10	40
$S_{ball}/\text{mass of sample (m}^2 \cdot \text{kg}^{-1})$	0.60		2.27		2.69	
Maximum kinetic energy delivered by the whole milling media/($S_{ball}/\text{mass of sample}$) (kWh.m ² .kg ⁻¹)	303		276		1.3	
Main mechanical stress imparted	Impact		Impact + Attrition		Attrition	

found to deliver the highest level of specific energy, whereas VBM delivered approximately 230 times less specific energy, with SBM again intermediate between RBM and VBM.

In a previous paper, Rajaonarivony et al. (2019) [33] showed through simulation experiments in a reciprocating small-scale ball mill that the share of impacts, among the multiple mechanical forces delivered by a mill, is proportional to the amount of kinetic energy imparted in the collisions between the milling bodies and the surface of the target sample. They also provided evidence that the share of attrition resulting from friction is directly related to the number of points of ball-to-matter collision. Applying these findings to the three ball mills studied here, it becomes apparent that the RBM works predominantly by impact, with a high ball energy and low number of ball-to-matter contact points, whereas the VBM works mostly by attrition, with a low specific energy and a large number of surface contacts. SBM is just behind RBM on collision energy and just behind VBM on ball-to-matter surface ratio. We thus concluded that the SBM works by a mixed impact/attrition regime, which is consistent with Mucsi & Rácz (2017) [24] who studied the grinding of red grapeseed residues in a similar stirred media mill.

3.2. Reproducibility of the milling process

Table 3 reports the milling times needed to attain the target particle size of 20 μm. Experiments were conducted twice, and a coefficient of variation on the specific surface area measured by laser diffraction for the two trials was calculated, as also reported in Table 3.

Note that the required milling times differ widely between mill systems. It takes more than 12 times longer to reach the target particle size in the RBM than in the SBM. The relative differences between the two milling experiments were in an acceptable range, with a maximum value of 10.6 indicating that the milling process showed fair reproducibility. The greatest variations were obtained with the faster milling device (SBM) for which a short time change can lead to greater surface-area differences in the milled powders.

3.3. Particle-size distributions of milled samples

Fig. 2 reports the mean cumulative particle size distributions of the two lignocellulosic powders ground in the three ball mills. As

Table 3
Reproducibility of the milling process.

	Bark		Straw	
	Milling time (h)	CoV (%)	Milling time (h)	CoV (%)
RBM	4.5	1.03	23	4.2
SBM	0.36	6.0	1.6	10.6
VBM	1.0	4.8	4.3	3.8

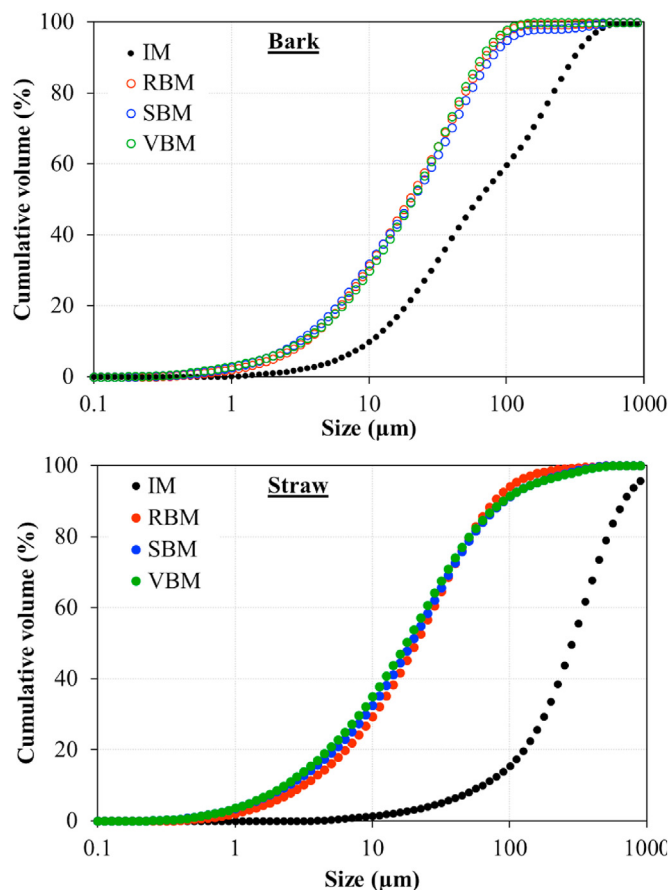


Fig. 2. Cumulative particle size distributions of IM-bark, IM-straw, and finely-milled bark and straw powders (median size = 20 μm) obtained from the three ball mills.

an indication, the particle size distributions of IM_bark and IM_straw pre-milled in the impact mill, that fed the three ball mills, were also reported in Fig. 2. The main particle size indicators are summarized in Table 4.

In all cases, the milling process employed was able to achieve a target particle size of $d_{50} = 20 \mu\text{m}$, and the particle size indicators were fairly similar between each system. The cumulative curves were very similar between powders from the three milling devices for both biomasses, with only a slight difference found for the cumulative distribution of RBM_straw, which was a little more centred on the median value compared to SBM_straw and VBM_straw (i.e. a higher d_{10} and a lower d_{90}). The d_{90} values obtained were slightly higher for straw than for bark. In general, the milling devices generating attrition tended to produce particles with higher d_{90} values. This was the case with the VBM (attrition as main mechanical stress) for bark and the VBM and the SBM (attrition and

Table 4
Size properties of IM-bark, IM-straw, and powders obtained from the three ball mills.

Bark	d10 (μm)	d50 (μm)	d90 (μm)
IM	10.2	62.7	309.0
RBM	3.4	19.7	68.6
SBM	3.3	20.6	65.5
VBM	3.1	20.6	76.1
Straw			
	d10 (μm)	d50 (μm)	d90 (μm)
IM	63.5	285.7	691.2
RBM	3.1	20.7	77.2
SBM	2.4	19.2	89.7
VBM	2.3	18.0	88.8

impact) for straw. However, these differences remain minor, and overall, we conclude that all three milling devices were able to produce powders that meet the specifications in terms of particle size distribution.

3.4. Specific milling time and energy consumption

In a first approach, the performance of a milling device can be evaluated through two parameters: (i) specific milling time, which is the time required to produce 1 kg of fine-powder lignocellulosic biomass (calculated as in Eq. (6)) and (ii) specific energy consumption (calculated as in Eq. (5)). Specific milling time is obtained by dividing the milling time by the mass processed (m_{sample}), and it informs on the milling process speed. Specific energy consumption is defined as the amount of energy used to mill 1 ton of biomass to the targeted particle size of 20 μm .

The specific milling times are reported in Table 5. Bark was milled 4 to 5 times faster than straw, depending on the device considered. Interestingly, this ratio was of the same order of magnitude as the ratio of the median particle size of IM_straw to median particle size of IM_bark, suggesting a strong correlation between size of input material and milling time.

Fig. 3 shows that E_s is much higher for straw milling than bark milling, which is related to the longer specific milling time needed for straw due to the input particle size and apparent density differences previously discussed.

For both biomasses, RBM had the longest milling time and so logically consumed more energy than SBM and VBM, i.e. about 4 times more for bark and 5–6.5 times more for straw, confirming that impact as main mechanical stress is less efficient than attrition or mixed (impact + attrition) mechanical stresses. Note too that the energy consumption for milling bark was not different between SBM ($4.2 \times 10^2 \text{ kWh.t}^{-1}$) and VBM ($4.0 \times 10^2 \text{ kWh.t}^{-1}$) whereas the energy consumption for milling straw was much lower with the SBM ($13.7 \times 10^2 \text{ kWh.t}^{-1}$) than the VBM ($17.4 \times 10^2 \text{ kWh.t}^{-1}$). We therefore find evidence that a mixed mechanical stresses is more efficient for fragmenting the fibrous-structured straw particles.

Table 5
Specific milling time of bark and straw in the three ball mills.

	t_s specific milling time (h.kg^{-1})	
	Bark	Straw
RBM	22.5	115
SBM	1.1	4.9
VBM	1.0	4.3

3.5. Rittinger model and grindability

To overcome the gap in initial particle size between IM_bark and IM_straw and eliminate the dependency on capacity differentials between the ball-mill devices, we plotted in Fig. 4 the created specific surface area, defined as the surface area at time t (SSA_t) minus the initial surface of IM_bark/straw (SSA_i), as a function of the specific energy consumed for different milling times (t). SSA_t and SSA_i were measured by laser diffraction (where SSA corresponds to the total surface area created by a given weight of powder and determined as the sum of particle surfaces in all size classes, based on the assumption of sphere-shaped particles [34]):

$$\text{Created specific surface area} = SSA_t - SSA_i$$

Fig. 4 shows a linear correlation for the results from all the milling devices on both biomasses, in agreement with the Rittinger model which states that grinding energy is directly proportional to created specific surface area [35]. The coefficient of this linear correlation is related to type of biomass and type of mill.

Overall, a milling process will be more efficient if there is a good fit between the mechanical stress employed and the type of material to mill. This fit dictates the 'grindability' of the materials in a given device. In a first approach, we assume that the slope of the linear correlation plots this 'grindability', which means that grindability is inversely proportional to specific energy consumption: easier-milling material will consume less specific energy.

In other words, by fitting the experimental data, the grindability is deduced from the following expression:

$$\text{Created specific area } (E_s) = \text{Grindability} * E_s$$

The final value of the created surface is higher for straw than for bark, because IM_straw has a lower the specific surface area than IM_bark.

This confirms the previous observations made on the basis of the specific energy consumption. Bark appears to have significantly better grindability than straw in all the milling devices. Bark and straw both have lower grindability values in RBM than in other devices. In addition, grindability values for bark were very similar between SBM (0.0016) and VBM (0.0015), whereas grindability values for straw were higher in the SBM than in the VBM. This confirms that mixed impact-plus-attrition is the most efficient regime for milling straw.

3.6. Agglomeration phenomena in the different milling devices

Unlike previous observations on the fine milling of wood [36], bark [33] or silica [34], the specific surfaces in Fig. 4 did not reach a plateau, which is generally attributed to a prevalence of agglomeration phenomena, in the range of E_s applied in these

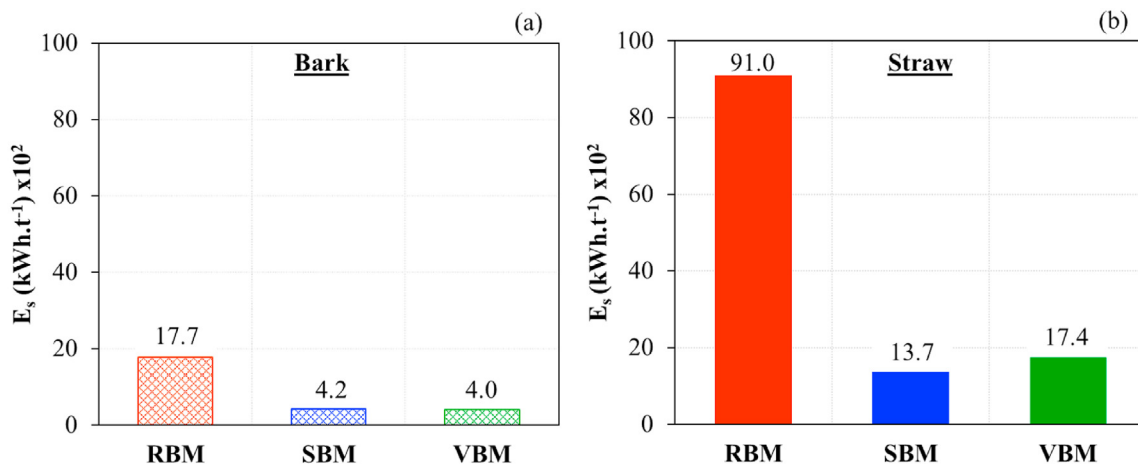


Fig. 3. Specific milling energy consumption (calculated from Eq. (5)) to obtain (a) bark and (b) straw powders of median size = 20 μm.

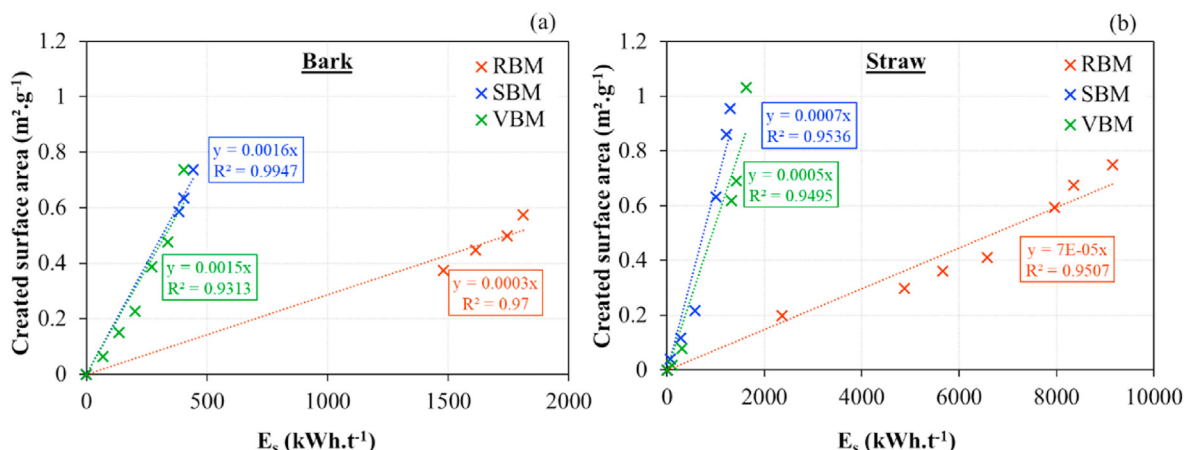


Fig. 4. Evolution of created specific surface area (from laser granulometry measurements) of (a) bark and (b) straw powders as a function of specific energy consumption.

experiments. The milling experiments may have not been long enough to attain a clear agglomeration plateau. The linear correlation observed appears to reflect a constant balance between comminution and agglomeration phenomena throughout the milling process. We previously made similar observations for flax fibres milled in the VBM [28]. However, the agglomeration phenomena may still be present but masked by course of comminution. In previous work, Rajaonarivony et al. (2019) [33] showed that the agglomeration phenomena was assessable by comparing the specific surface areas measured by laser diffraction and by gas sorption (BET). These values, are reported in Table 6 for both of the biomasses.

Direct comparison of SSA between laser diffraction and BET is not a trivial task, as the two measurement methods are based on different physical principles. In particular, the difference between

SSA_{BET} and SSA_{granulo} is much higher for straw than for bark, probably due to a higher porosity of straw [37]. However, for a given biomass, it is instructive to qualitatively compare the SSA_{BET}-to-SSA_{granulo} ratio for the different devices in order to evaluate the potential agglomeration state of the powder, as the devices that lead to high ratios can be considered to generate more agglomeration. For both biomasses, the milling devices ranked similarly from the highest to lowest ratio, i.e. VBM, RBM and SBM. Rajaonarivony et al. (2019) [33] evidenced that attrition generated a high amount of small particles, which could logically lead higher agglomeration levels. They also demonstrated that the impact work tends to create stronger agglomerates by compacting the powder, which is consistent with our observations that the RBM leads to intermediate-level agglomeration whereas the SBM remained the ‘least agglomerative’ device.

Table 6 Specific surface areas of finely-milled powders measured by laser granulometry (SSA_{granulo}) and by gas sorption (SSA_{BET}) techniques, and SSA_{granulo}-to-SSA_{BET} ratio.

	Bark			Straw		
	SSA _{granulo} (m ² .g ⁻¹)	SSA _{BET} (m ² .g ⁻¹)	SSA _{BET} /SSA _{granulo}	SSA _{granulo} (m ² .g ⁻¹)	SSA _{BET} (m ² .g ⁻¹)	SSA _{BET} /SSA _{granulo}
RBM	0.82 ± 0.10	1.27 ± 0.01	1.55	0.83 ± 0.10	2.24 ± 0.08	2.70
SBM	0.95 ± 0.03	1.14 ± 0.06	1.20	1.08 ± 0.00	2.48 ± 0.03	2.30
VBM	0.92 ± 0.00	1.61 ± 0.06	1.75	1.11 ± 0.01	3.21 ± 0.03	2.89

3.7. Energy utilization

Apparent energy consumption for comminution (calculated from SSA_{granulo}) can be affected by the degree of powder agglomeration imparted by the different mills, as the fine particles that agglomerate are not detected in the total surface area measured by laser diffraction.

Fig. 5 shows the energy utilization (U_e), *i.e.* the surface created by an input of 1 kWh, determined from both SSA_{granulo} and from SSA_{BET} [24]. This representation once again highlights the greater grindability of bark compared to straw, as a greater surface is created for 1 kWh input. The SSA measurement method also finds some major differences between milling devices.

First, note that the RBM had the lowest U_e values for both biomasses and both SSA measurement methods. This means that despite being widely used for milling biomass [21,38,39], the impact-regime RBM appears to be the least efficient device.

For bark, both measurement methods led to similar U_e values except in the case of VBM for which the U_e value determined by the BET method was 1.8 times higher than the U_e value obtained for the SBM. Indeed, the VBM, which mainly uses attrition, generated high numbers of fine particles that tend to agglomerate during milling but are still present in the final powder. These agglomerates of fines may increase the reactivity of the powder if they are de-agglomerated before or during application (for example, during the explosion of powdered fuel in an engine). For straw, there was a clear difference between the U_e values determined by laser diffraction and the BET method and can be directly correlated to the higher SSA value obtained with BET measurements. For both measurement methods, the U_e of the SBM and VBM were in the same range. We had previously shown that a combination of impact and attrition allows a faster and a more efficient reduction of fibrous particles, but the ability of attrition to produce large amounts of small particles that tend to agglomerate partly compensates for this phenomenon and leads to similar efficiencies in SBM and VBM.

These conclusions warrant careful interpretation. On the one hand, agglomerates may not be disintegrated prior to or during application, which could prove prejudicial for end-product quality, whether for energy applications if a part of the surface is not accessible to the oxidizing reaction, or for material applications if the agglomerates induce structural weaknesses. On the other hand, if agglomeration is kept limited during the milling step, such as by grinding aids, then milling efficiency could be significantly increased, as the energy delivered by the device will only be used to fragment the raw material and not to de-agglomerate the powder or even drive the formation of new agglomerates by compaction [40].

Therefore, choosing the right milling device is never a trivial task, and should be done carefully by factoring in the energy efficiency of the mill but also the quality of the powder for the targeted application. The following discussion aims to provide key insights to guide the choice of suitable milling hardware for lignocellulosic biomass comminution.

4. Discussion

The results of this study demonstrate that fine-milling performances on lignocellulosic feedstock can differ according to technology employed and type of processed biomass. First, note that for most of the biomasses available, a single milling step is unable to reach the 10–20 μm particle size range. Pre-milling steps are required to render the format of the input biomass material compatible with proper functioning of the last comminution step, that can be viewed as a finishing milling. However, some other commonly-available small-particulate-format feedstocks such as rice husk or wood sawdust may be fed directly into ball mills to yield ultrafine powders.

In order to compare the three ball mills in terms of performance and practicality in lignocellulosic biomass milling, we assessed their productivity and speeds using two indicators, *i.e.* mass productivity (P_m) and surface creation rate (R_s), calculated according to equations (8) and (9). P_m corresponds to the mass of powder with a median particle size $d_{50} = 20 \mu\text{m}$ that can be produced per kWh delivered by the machines, and R_s is an expression of the speed of surface creation, *i.e.* the variation in specific surface area (measured by the BET method) that is generated per hour. P_m gives an indication of how efficiently the available power is used in the different milling machines, and R_s gives an indication of their time efficiency. The indicators for bark and straw milling are given separately. Furthermore, average values were calculated to give a representative estimate for lignocellulosic biomass in general. Indeed, bark and straw were chosen in this study for their very different compositional and mechanical typologies that span the potential milling behaviour of a wide range of current lignocellulosic feedstocks. Table 7 reports the values for maximum available specific power (nominal machine power relative to 1 kg of process capacity in the mill).

The most powerful mill is clearly the SBM, with ~ 2.5 times more available power than the RBM and up to 15 times more available power than the VBM, bearing in mind that this power is applied through different dominant mechanical stresses in the three milling devices. The average mass productivity on biomass was similar between the SBM and VBM, whereas the RBM performed poorly (P_m was ~ 4.5 times lower than with the SBM and VBM). We conclude that the available power is much better utilized in the

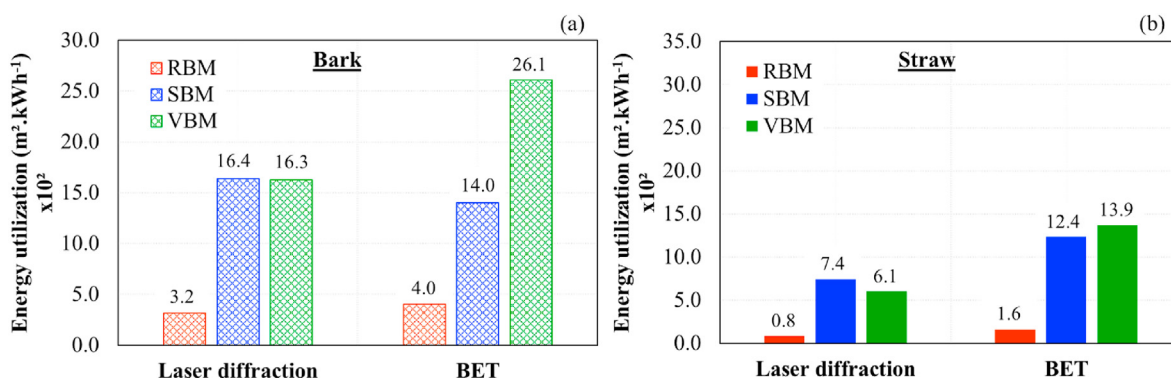


Fig. 5. Energy utilization of the ball mills, using the SSA_{granulo} and SSA_{BET} values calculated for (a) bark and (b) straw.

Table 7
Available power, mass productivity and surface creation rate of the three ball-mills.

	Available specific power ($\text{kW}\cdot\text{kg}^{-1}$) P_m : Mass productivity ($\text{kg}\cdot\text{kWh}^{-1}$) (for $d_{50} = 20 \mu\text{m}$ powder)			R_s : Surface creation rate ($\text{m}^2\cdot\text{g}^{-1}\cdot\text{h}^{-1}$) (calculated from SSA_{BET})		
	Bark	Straw	Average	Bark	Straw	Average
RBM 1.9	0.56	0.11	0.34	0.15	0.06	0.11
SBM 4.6	2.34	0.73	1.53	1.54	1.04	1.29
VBM 0.3	2.50	0.57	1.54	1.03	0.56	0.79

VBM (working predominantly by attrition) and the SBM (working predominantly by impact + attrition) compared to the RBM (working predominantly by impact). Looking at the two biomass samples separately, it can be seen that there is a gap in productivity between bark and straw in each mill. Whatever the milling device employed, P_m was 3–5 times higher for bark, with the biggest performance gap found for the RBM (impact regime). The mechanical properties of the brittle pine bark make it more conducive to milling than straw which has a deformability that absorbs a larger share of the milling power. In the SBM, the productivity difference between bark and straw was smallest, thus evidencing the efficiency of combined impact + attrition processes on recalcitrant fibrous material. The average processing speed (R_s) of the mills shows that SBM enables far more rapid surface-area creation than the RBM (12 times) but only 1.6-times faster surface-area creation than the VBM. Surface-area creation was always quicker for bark than for straw, whatever the mill. The processing-speed difference between bark and straw was biggest in the RBM and smallest in the SBM.

In summary, this study suggests that fine milling of lignocellulosic biomass in batch ball mills is more efficient when using machines that work mainly by attrition or impact + attrition than machines that work mainly by impact. A mill combining impact and attrition stresses proves more efficient in terms of productivity and processing speed when the biomass to be milled is recalcitrant, fibrous and tenacious, like straw. However, the faster processing speed of an SBM-type mill comes at a cost of high power demand, as seen in Table 7. Mucsi & Racz (2017) [24] also demonstrated that a stirred-bead mill resembling our SBM, which they called a ‘high energy density mill,’ was highly efficient for the ultrafine dry comminution (10 μm range) of grapeseed, which is a tenacious and multi-layered lignocellulosic material. On the other hand, a VBM-type mill uses less electric power to achieve effective fine powder production with good power utilization, but with longer processing times. Kobayashi et al. (2007) [5] showed that a vibratory mill is better designed than cutter mills or refiners for pulverizing lignocellulosic biomass. They reported values in the range of 400 $\text{kWh}\cdot\text{t}^{-1}$ to reach particle sizes down to a few dozen μm , which is comparable with our data on bark milling with the VBM. They successfully converted spruce tree shavings into 20–30- μm powders using their vibration mill, but they also noted significant agglomeration with this type of technology. An RBM-type mill appears ill-suited to lignocellulosic biomass pulverization, in terms of energy utilization, productivity and processing speed, with the parameters used in our study. Using the RBM milling principle for biomass micronization would entail restudying the operating parameters, the mass and shape of the balls, and possibly even the geometry of the milling chamber. Although our results were obtained at relatively small scale, we can assume that our analysis of the comminution mechanisms and energy utilization ranges of the different mill types compared here remains valid at higher scale, and could thus inform the selection of machine configurations for larger processing capacities.

Another important factor when milling lignocellulosic biomass

is the energy-effectiveness of the process, especially when combustion applications are targeted. The energy spent for particle size reduction should not exceed the basic energy content (expressed as lower heating value, LHV) of the biomass. Bark and straw have LHVs of 4700 and 4100 $\text{kWh}\cdot\text{t}^{-1}$, respectively. The milling energies in our study ranged from 400 $\text{kWh}\cdot\text{t}^{-1}$ for bark milled with the VBM to more than 9000 $\text{kWh}\cdot\text{t}^{-1}$ for straw milled with the RBM. The most advantageous situations were for bark processed by SBM and VBM devices, where milling energy represents less than 10% of LHV whereas straw processed with the same mills required an input demand of 33–42% of its basic energy content. Milling with the impact-regime RBM, in the configuration used in this work, was by far the less viable process route, as it demanded 37% of the bark energy content and as high as 220% of the straw energy content to reduce these materials into 20 μm powders. RBM technology is clearly not adapted to deep comminution of fibrous lignocellulosics. Concerning the other mills, even though the energy required for extensive milling may in some cases appear relatively high compared to the potential heat release of the biomass, it must be born in mind that there is plenty of room for improving and optimizing energy utilization when upscaling the process. For example, industrial wheat grain processing now requires as little as 50 $\text{kWh}\cdot\text{t}^{-1}$ to mill flour [36].

The superfine powdered format confers unique fuel properties to the dry biomass. Controlled powder explosivity, which can only be reached below a certain particle size, can ‘fuel’ internal combustion engines that are able to instantly deliver substantial mechanical power. The energy services provided by the lignocellulosic biomass can thus be extended far beyond the conventional products of slow combustion and gasification.

5. Conclusion

This experimental research studied two different lignocellulosic biomasses milled in batch ball mills operating in three different functional configurations. The results showed that the milling stresses were transferred mainly by impact in the rotary ball mill (RBM), by attrition in the vibratory ball mill (VBM), and by a combination of impact and attrition in the stirred ball mill (SBM). In each mill type, the particle size reduction was always quicker and less energy-intensive on bark (a brittle material) than on straw (an elastoplastic material). Among the three mills, the RBM required the longest milling times and was the least energy-efficient. The SBM and VBM showed comparable energy utilization, but the VBM caused significantly more agglomeration of fines. The SBM processed the matter faster than the other devices and was proportionally more efficient on the fibrous lignocellulosic sample, thus providing evidence that a combination of attrition and impact stresses is more effective for the pulverization of lignocellulosic biomass.

Besides the efficiency of the milling process, another key factor for driving the use of lignocellulosic biomass is that the milled biomass powders can meet the specifications required for end-use applications. The milling step should be managed and controlled to

ensure that the powdered product exhibits specified individual and collective particle properties, i.e. particle size and dispersion and particle shapes, resulting in suitable and reproducible behaviour in terms of storage and functional and flow properties. The powders obtained from the three ball mills studied here now need to be thoroughly characterized in order to relate their properties to the powder process technology used.

Credit author statements

Rouau X, Conceptualization: Formal analysis: Project administration: Supervision: Writing – original draft Writing – review & editing: Mayer-Laigle C, Conceptualization: Formal analysis: Writing – original draft Writing – review & editing: Piriou B; Conceptualization: Project administration: Validation: Writing – review & editing: Rajaonarivony K. R; Data curation: Formal analysis: Investigation: Methodology: Writing – original draft Writing – review & editing:

Declaration of competing interest

The authors declare that they have no known competing financial interests or personal relationships that could have appeared to influence the work reported in this paper.

Acknowledgement

The authors thank the PLANET facility (doi: 10.154541.5572338990609338E12) run by the IATE joint research unit for providing valuable process experiment support. The authors also acknowledge the French national research institute for Agriculture, Food and Environment (INRAE) for supporting this research work.

References

- [1] Büyükkökan G, Karabulut Y, Mukul E. A novel renewable energy selection model for United Nations' sustainable development goals. *Energy* 2018;165: 290–302. <https://doi.org/10.1016/j.energy.2018.08.215>.
- [2] International Energy Agency. Fuels and technologies – renewables. <https://www.iea.org/fuels-and-technologies/renewables>. [Accessed 28 February 2021].
- [3] Dale B. Time to rethink cellulosic biofuels? *Biofuel Bioprod Biorefin* 2018;12: 5–7. <https://doi.org/10.1002/bbb.1856>.
- [4] Lynd LR. The grand challenge of cellulosic biofuels. *Nat Biotechnol* 2017;10: 912–5. <https://doi.org/10.1038/nbt.3976>.
- [5] Kobayashi N, Guilin P, Kobayashi J, Hatano S, Itaya Y, Mori S. A new pulverized biomass utilization technology. *Powder Technol* 2008;180(3):272–83. <https://doi.org/10.1016/j.powtec.2007.02.041>.
- [6] Mcknight JK, Mcknight JT. Powdered fuels, dispersions thereof, and combustion devices related thereto. U.S. Patent No. 2015;9(57):522. 16 Jun.
- [7] Piriou B, Vaitilingom G, Veyssi re B, Cuq B, Rouau X. Potential direct use of solid biomass in internal combustion engines. *Prog Energy Combust Sci* 2013;39(1):169–88. <https://doi.org/10.1016/j.peccs.2012.08.001>.
- [8] Stover L, Piriou B, Vaitilingom G, Rouau X. The biomass dust-fueled engine. 26. Copenhagen, Denmark: European Biomass Conference and Exhibition (EUBCE); May 2018.
- [9] Stover L, Piriou B, Caillol C, Higelin P, Proust C, Rouau X, Vaitilingom G. Direct use of biomass powder in internal combustion engines. *Sustainable Energy & Fuels* 2019;3(10):2763–70. <https://doi.org/10.1039/C9SE00293F>.
- [10] Eckhoff RK. Dust explosions in the process Industries: Identification, Assessment and control of dust Hazards. Gulf Professional Publishing, Elsevier; 2003.
- [11] Abbasi T, Abbasi SA. Dust explosions—Cases, causes, consequences, and control. *J Hazard Mater* 2007;140(1–2):7–44. <https://doi.org/10.1016/j.jhazmat.2006.11.007>.
- [12] Tymoszuk M, Mroczek K, Kalisz S, Kubiczek H. An investigation of biomass grindability. *Energy* 2019;183:116–26. <https://doi.org/10.1016/j.energy.2019.05.167>.
- [13] Mayer-Laigle C, Rajaonarivony R, Blanc N, Rouau X. Comminution of dry lignocellulosic biomass: Part II. Technologies, improvement of milling performances, and security issues. *Bioengineering* 2018;5(3):50. <https://doi.org/10.3390/bioengineering5030050>.
- [14] Gravelins RJ. Studies of grinding of wood and bark-wood mixtures with the Szego mill. PhD Thesis. National Library of Canada; 1999.
- [15] Kokko L, Tolvanen H, H m l inen K, Raiko R. Comparing the energy required for fine grinding torrefied and fast heat treated pine. *Biomass Bioenergy* 2012;42:219–23. <https://doi.org/10.1016/j.biombioe.2012.03.008>.
- [16] Jafari Naimi L. A study of cellulosic biomass size reduction. PhD Thesis. University of British Columbia; 2016.
- [17] Monov V, Sokolov B, Stoenchev S. Grinding in ball mills: modeling and process control. *Cybern Inf Technol* 2012;12(2):51–68. <https://doi.org/10.2478/cait-2012-0012>.
- [18] Becker M, Kwade A, Schwedes J. Stress intensity in stirred media mills and its effect on specific energy requirement. *Int J Miner Process* 2001;61(3): 189–208.
- [19] Breitung-Faes S, Kwade A A. Prediction of energy effective grinding conditions. *Miner Eng* 2013;43:36–43.
- [20] Samanli S,  uhadaroglu D, Kizgut S. Comparison of grinding performance between stirred mill and ball mill. *J Ore Dress* 2008;10:24–9.
- [21] Williams O, Newbolt G, Eastwick C, Kingman S, Giddings D, Lormor S, Lester E. Influence of mill type on densified biomass comminution. *Appl Energy* 2016;182:219–31. <https://doi.org/10.1016/j.apenergy.2016.08.111>.
- [22] Mucsi G. Grindability of quartz in stirred media mill. *Part Sci Technol* 2013;31(4):399–406. <https://doi.org/10.1080/02726351.2013.767294>.
- [23] Dumas C, Silva Ghizzi Damasceno G, Barakat A A, Carr re H, Steyer J-P, Rouau X. Effects of grinding processes on anaerobic digestion of wheat straw. *Ind Crop Prod* 2015;74:450–6. <https://doi.org/10.1016/j.indcrop.2015.03.043>.
- [24] Mucsi G, R cz A. Grinding kinetics of red grape seed residue in stirred media mill. *Adv Powder Technol* 2017;28(10):2564–71. <https://doi.org/10.1016/j.apt.2017.07.007>.
- [25] Fabre C, Buche P, Rouau X, Mayer-Laigle C. Milling itineraries dataset for a collection of crop and wood by-products and granulometric properties of the resulting powders. *Data in Brief* 2020;33:106430. <https://doi.org/10.1016/j.dib.2020.106430>.
- [26] AOAC. Official. Methods of analysis. eighteenth ed. Arlington, VA, USA: Association of Official Analytical Chemist; 2005.
- [27] Francioli D. Effect of operational variables on ball milling. PhD Thesis; 2015.
- [28] Mayer-Laigle C, Bourmaud A, Shah DU, Follain N, Beaugrand J. Unravelling the consequences of ultra-fine milling on physical and chemical characteristics of flax fibres. *Powder Technol* 2020;360:129–40. <https://doi.org/10.1016/j.powtec.2019.10.024>.
- [29] Merkus HG. Laser diffraction, particle size measurements: Fundamentals, practice, quality. Dordrecht: Springer Netherlands; 2009.
- [30] Rouquerol J, Rouquerol F, Llewellyn P, Maurin G, Sing KSW. Adsorption by powders and porous solids: principles, methodology and applications. Elsevier Science; 2013.
- [31] M thode de d termination du pouvoir calorifique. Norme XP CEN/TS 14918; 2012.
- [32] Fuerstenau DW, Abouzeid A-Z. The energy efficiency of ball milling in comminution. *Int J Miner Process* 2002;67(1):161–85.
- [33] Rajaonarivony K, Rouau X, Lampoh K, Delenne J-Y, Mayer-Laigle C. Fine comminution of pine bark: how does mechanical loading influence particles properties and milling efficiency? *Bioengineering* 2019;6(4):102. <https://doi.org/10.3390/bioengineering6040102>.
- [34] Blanc N, Mayer-Laigle C, Frank X, Radjai F, Delenne J-Y. Evolution of grinding energy and particle size during dry ball-milling of silica sand. *Powder Technol* 2020;376:661–7. <https://doi.org/10.1016/j.powtec.2020.08.048>.
- [35] Charles RJ. Energy-size reduction relationships in comminution. *Transactions of AIME. Mining Engineering* 1957:80–8.
- [36] Karinkanta P,  mm l  A, Illikainen M, Niinim ki J. Fine grinding of wood – overview from wood breakage to applications. *Biomass Bioenergy* 2018;13: 31–44. <https://doi.org/10.1016/j.biombioe.2018.03.007>.
- [37] Chesson A, Gardner PT, Wood TJ. Cell wall porosity and available surface area of wheat straw and wheat grain fractions. *J Sci Food Agric* 1997;75(3): 289–95. [10.1002/\(SICI\)1097-0010\(199711\)75:3<289::AID-JSFA879>3.0.CO;2-R](https://doi.org/10.1002/(SICI)1097-0010(199711)75:3<289::AID-JSFA879>3.0.CO;2-R).
- [38] Barakat A, Mayer-Laigle C, Solhy A, Arancon RAD, de Vries H, Luque R. Mechanical pretreatments of lignocellulosic biomass: towards facile and environmentally sound technologies for biofuels production. *RSC Adv* 2014;89: 48109–27. <https://doi.org/10.1039/C4RA07568D>.
- [39] Kim HJ, Chang JH, Jeong B-Y, Lee JH. Comparison of milling modes as a pretreatment method for cellulosic biofuel production. *Journal of Clean Energy Technologies* 2013;45–8. <https://doi.org/10.7763/JOCET.2013.V1.11>.
- [40] Hennart SLA, van Hee P, Drouet V, Domingues MC, Wildeboer WJ, Meesters GMH. Characterization and modeling of a sub-micron milling process limited by agglomeration phenomena. *Chem Eng Sci* 2012;71:484–95. <https://doi.org/10.1016/j.ces.2011.11.010>.